BIBECHANA
Vol. 22, No. 1, April 2025, 73-79

ISSN 2091-0762 (Print), 2382-5340 (Online)
Journal homepage: http://nepjol.info/index.php/BIBECHANA
Publisher:Dept. of Phys., Mahendra Morang A. M. Campus (Tribhuvan University)Biratnagar

Fabrication of Cu: ZnO thin film sensor for ethanol vapor detection

Rabin Simkhada[1], Dalton R. Gibbs[2], Soma Dhakal[2], Dipak Oli[1], Rishi Ram Ghimire[3], Deependra Das Mulmi[4,*], Leela Pradhan Joshi[1,*]

[1]*Dept. of Physics, Amrit Campus, Tribhuvan University, Kathmandu, Nepal*
[2]*Virginia Commonwealth University, Dept. of Chemistry, Richmond, VA, 23284, USA*
[3]*Dept. of Physics, Patan Multiple Campus, Tribhuvan University, Kathmandu, Nepal*
[4]*Nanomaterials Research Laboratory,*
Nepal Academy of Science & Technology, Khumaltar, Nepal
*Corresponding author. Email: deependra.mulmi@nast.gov.np(DM)
leela.pradhanjoshi@ac.tu.edu.np(LP)

Abstract

For a long time, metal oxide semiconductor (MOS) based gas sensors have been widely used in domestic, commercial, and industrial sectors to detect harmful gases. The performance of such sensors is significantly enhanced by appropriate doping of suitable materials into MOS such as ZnO and SnO_2. This work showcases the design, analysis, and use of a Cu-doped ZnO (Cu: ZnO) film tailored for detecting traces of ethanol vapor at lower temperatures. Herein, various Cu: ZnO films have been fabricated on glass substrates using a spin coater followed by annealing at 600 ^0C for 1 hour in a muffle furnace. So-prepared samples have been characterized using X-ray diffraction, Energy Dispersive Analysis X-ray (EDAX), UV-visible spectrophotometer, and Scanning Electron Microscopy (SEM). The XRD analysis showed a polycrystalline nature with preferred orientation along (100) and (002) crystal planes. The morphology study showed their porous and granular surface structure. These films' elemental analysis demonstrated the good incorporation of Cu into the ZnO matrix. The UV-visible results showed a significant decrease in the band gap from 3.28 eV for undoped ZnO to 3.20 eV for Cu: ZnO films. Ultimately, as-prepared Cu: ZnO thin films were used for sensing ethanol vapor at temperatures ranging from 100 ^0C to 300 ^0C. The result showed a maximum sensitivity of 70.60 ^0C at a reduced temperature of 140 ^0C at 4% Cu: ZnO thin, which implies that Cu: ZnO is suitable for developing the gas sensors for upcoming future generations.

Keywords
Polycrystalline, Spin coating, Gas sensor, Metal oxide semiconductor.

Article information
Manuscript received: October 6, 2024; Revised: January 13; Accepted: January 17, 2025
DOI https://doi.org/10.3126/bibechana.v22i1.70639

1 Introduction

Over the last few decades, the rapid increase of the global population has exploited excessive non-renewable natural resources, which produce numerous harmful gases [1, 2]. It has become one of the greatest environmental risks to health [3]. If the normal concentration of these gases exceed, then they cause long-term health hazards to people that may lead to heart disease, lung cancer, and respiratory infections [4–6]. So, there is an instant need for effective gas sensors to detect and reduce these problems. Several devices are available for tracking pollutants and dangerous gases, which are very expensive, time-consuming, and hardly used in real-time situations. To reduce the above- mentioned problems, there is a greater demand for cost-effective, accurate, portable, and reliable gas sensors. In recent times, several metal oxide semiconductors have been used to detect pollutant gases and organic vapor including ZnO, TiO_2, Fe_2O_3, SnO_2, $MgAl_2O_4$, $CuTiO_2$, and many more [7–9]. Among these, ZnO has been considered one of the most promising materials for detecting toxic gases as it has a wide band gap, high exciton energy, chemical stability, more electron mobility, a high surface area, and is nontoxic and abundant in nature. [10–14]. Most ZnO sensors follow the surface-controlled sensing mechanism. Nonetheless, there are still certain problems with gas sensitivity, such as high operating temperatures, huge response and recovery times, and poor sensitivity percentages of gas response. Fabrication of ZnO gas sensors with very good sensitivity and selectivity for spotting toxic and explosive gas leakages is a major challenge, mainly because of their high operating temperatures [15]. So, it is critical to discover a practical method for creating ZnO nanostructures with high sensitivity and superior stability [16]. Doping of the metal is frequently used to enhance the sensing behavior of the metal oxide semiconductors (MOS) [17]. In this work, copper is doped in a different weight ratio into ZnO over a glass substrate. Copper (Cu) is known for its excellent electrical and thermal conductivity, ductility, and resistance to corrosion [18]. Cu doped ZnO exhibits properties that are favorable for sensing [19, 20]. The most popular and inexpensive type of alcohol, ethanol, is widely used in the chemical industry, brewing, medicine, pharmaceuticals, personal care products, fuel, and laboratory [4, 21]. Long term use and high dose exposure of ethanol cause a weakened immune system, and lead- to health hazards to living beings. There is an urgent need for the detection of such lethal gases with effective sensing materials. This work reports on the synthesis of undoped and Cu doped ZnO for detecting traces of ethanol vapor at reduced temperatures than reported values. There is a significant challenge in establishing a stable device using any oxide material due to the physisorption and chemisorption of moisture from the atmosphere, which gradually degrades the quality of the films and changes the performance of the device. To avoid this practical limitation, the device can be kept in a vacuum before use; however, this restricts and limits its application. Selectivity is a major challenge for this device. For example, the device responds to various alcohols (ethanol, methanol, butanol), water vapor, and ammonia. Therefore, the solution is to identify a selective dopant that can capture only certain types of molecules. Mass production using a low-cost chemical method is suitable, but it still lacks reproducibility. This limitation can be mitigated using vacuum techniques like PLD, sputtering, or thermal evaporation; however, the cost would be high for mass production. Once the selectivity of the device towards the target molecules is achieved, the application becomes feasible, and at least a disposable, low-cost device can be made using a simple chemical method. This research is beyond the scope of mass production; it focuses solely on how the Cu dopant changes the responsivity of the device to ethanol vapor.

2 Experimental Details

2.1 Materials

The materials used to fabricate Cu: ZnO films were copper chloride dihydrate, zinc acetate dihydrate, ethanol, labolene, acetone and distilled water. All the chemicals used in this experiment were of analytical grade.

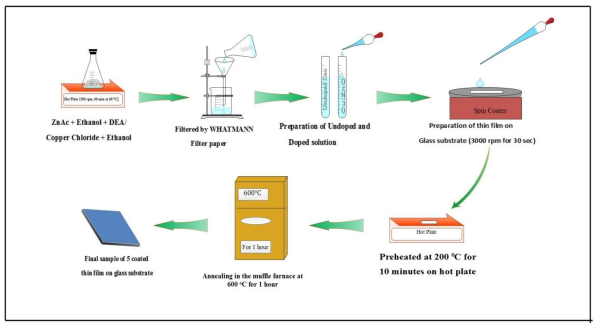

Figure 1: Schematic diagram for ZnO film preparation.

2.2 Deposition of ZnO film

Thin films of 0.5M undoped and Cu-doped ZnO were synthesized using a spin coater. The zinc acetate dihydrate salt dissolved in ethanol, while copper chloride was dissolved in ethanol solution separately. These two solutions were added and stirred for 60 minutes at 60 ^{0}C in a magnetic stirrer. Five

solutions were prepared without doping and varying Cu from 1% to 4% as a dopant. These solutions were left to age for 24 hours at room temperature before film deposition. Microscopic glass substrates were first cut into an appropriate size, then cleaned using labolene and acetone, and finally rinsed with distilled water. Subsequently, they were dried in a hot air oven at 150 ^{0}C for 2 hours. The speed and spinning time of the spin coater were set to 3000 rpm for 30 seconds. This process yielded undoped and Cu: ZnO layers of 1%, 2%, 3%, and 4% concentration on the glass substrate.

2.3 Characterization

Structural characteristics of as-prepared thin film were characterized by using X-ray diffractometer (XRD). Interplanar spacing (d) is calculated by using Bragg's law [22]

$2dsin\theta = n\lambda$

where, λ is the wavelength of the X-ray, n and θ represent order of diffractions and Bragg's angle, respectively. Further, average crystallite size (D) was computed using the relation of Debye–Scherrer formula [23]

$$D = \frac{0.9\lambda}{\beta Cos\theta}$$

where β represents the FWHM of the sharp peak. The surface morphology and elemental analysis of the undoped and Cu: ZnO was studied using Scanning Electron Microscopy (SEM) and Energy dispersive X-ray (EDAX). On the other hand, optical properties of ZnO and Cu: ZnO were investigated using UV- Visible spectrophotometer (Cary 60, Agilent Technology). The optical band gap energy of the thin films can be found by extending the linear segment of $(\alpha h\nu)^2$ on the x-axis. The formula employed for calculating the band gap is provided as follows:

$\alpha h\nu = A(h\nu \pm E_p - E_g)^n$

where A is a constant, h is the Planck constant, ν is the frequency of radiation and n is a constant that determines the type of the optical transition. Similarly, the sensitivity of thin films was evaluated by using formula [24]

$$S = \frac{R_a - R_e}{R_a} \times 100\%$$

where R_a is the resistance of thin film measured in the air and R_e is the resistance of thin film measured at ethanol vapor exposure.

3 Results and Discussion

3.1 Scanning Electron Microscopy

Scanning Electron Microscopy [25] is important as it helps for better understanding of surface textures of as prepared samples by providing high-resolution images. Figures [2] (a), (b), (c),(d) and (e) show the SEM images of undoped ZnO, 1%, 2%, 3%, and 4% Cu doped films at resolution of 500 nm, respectively. These SEM images clearly showed a grainy-like structure with a decrease in particle size for Cu: ZnO films. Insets in each figure show the SEM images captured at 100 nm resolution.

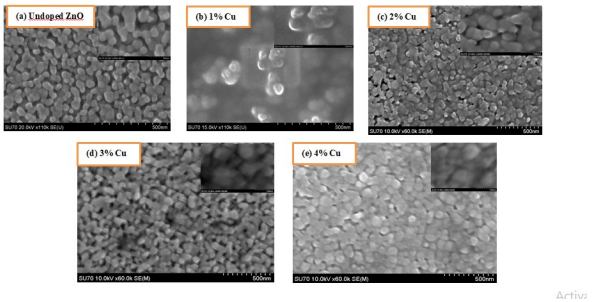

Figure 2: SEM images of (a) Undoped ZnO (b) 1% Cu: ZnO (c) 2% Cu: ZnO (d) 3% Cu: ZnO (e) 4% Cu: ZnO.

3.2 Energy Dispersive X-ray Analysis

EDAX is generally used for elemental analysis of prepared materials [26]. Here, the different elements present in as-prepared thin films are analyzed. Figure [3] (a) and (b) demonstrate the EDAX spectra of undoped and 1% Cu: ZnO thin films, respectively. The results show the presence of Zn, O along with traces of other elements of C, Si, and Ca are presented in the inset of Figure [3] (a). Figure [3](b) illustrates EDAX of Cu: ZnO. In this case, the atomic percentage of copper is quantified as 1.91% in the 1% Cu thin film. EDAX confirms the successful incorporation of Cu into the ZnO lattice and provides quantitative elemental composition. An optimal Cu concentration ensures improved sensor performance, while excessive doping can introduce defects that degrade conductivity and response stability.

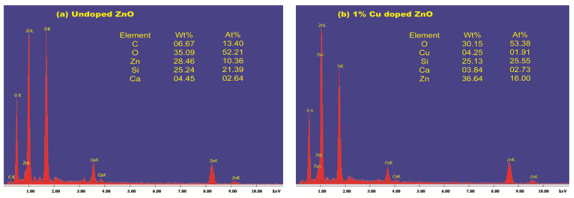

Figure 3: (color online) EDAX spectrum of: (a) undoped ZnO and (b) 1% Cu doped ZnO.

3.3 Structural Analysis

The surface morphology and grain size of the ZnO nanostructure play a major role in sensing and detection of gases. The structural analysis of undoped

and doped ZnO was performed by X-ray diffraction. The X-ray diffraction (XRD) pattern consists of a number of peaks indicating ZnO films were polycrystalline in nature. Figure [4] depicts the XRD pattern of ZnO with different concentrations of Cu ranging from 0% to 4%. Three intense peaks were observed at 33.19 ^{0} (100), 35.86 ^{0} (002) and 37.68 ^{0} (101) for undoped ZnO thin film that were found to be consistent with the ZnO peaks of JCPDS values.

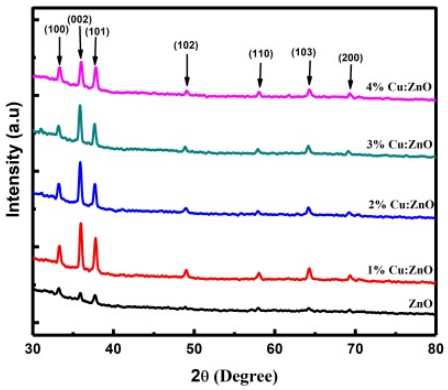

Figure 4: (color online) XRD pattern for undoped and Cu doped ZnO thin film.

Table 1: Comparison between the calculated interspacing distance (d), standard JCPDS d-spacing, and corresponding crystallite size.

Cu-ZnO (2θ) (°)	Calculated d (Å)	JCPDS d (Å)	Crystallite Size D(Å)	Average D (nm)	%
0%					
33.19	2.6978	2.8142	279.60	28.17	
35.86	2.5027	2.6033	329.39		
37.68	2.3859	2.4759	236.02		
1%					
33.28	2.6950	2.8142	281.76	26.09	
35.93	2.4960	2.6033	241.68		
37.76	2.3812	2.4759	259.32		
2%					
33.20	2.6968	2.8142	274.61	26.06	
35.86	2.5028	2.6033	243.25		
37.67	2.3864	2.4759	263.98		
3%					
33.16	2.6998	2.8142	256.09	26.47	
35.82	2.5047	2.6033	273.14		
37.64	2.3841	2.4759	265.13		
4%					
32.51	2.7525	2.6882	260.70	23.90	
35.18	2.5498	2.4952	225.23		
36.97	2.4302	2.3797	233.79		

The XRD major peaks observed were well aligned along the growth direction implies wurtzite structure of ZnO with no observable defects. Additionally, other minor peaks are also found in XRD patterns. These results vividly agree with the previously reported work [27–30]. Table [1] shows a comparison between the calculated interplanar spacing distance (d), standard JCPDS d-spacing and the corresponding crystalline size (D). The calculated value of d is compared with the standard JCPDS card number of 36-1451 [31]. The calculated value of interplanar spacing is found to be less than the JCPDS value, which may be due to the impurities in ZnO. The average crystallite sizes were of 28.17 nm, 26.09 nm, 26.06 nm, 26.47 nm, and 23.90 nm for undoped,1%, 2%, 3%, and 4% of Cu doped ZnO, respectively. Notably, these results vividly agree with the SEM results. Table 1 clearly shows the decreasing D value for Cu doped ZnO.

3.4 Optical Analysis

The optical band gap of thin films was calculated from Tauc plot. Figure [5] illustrates the band gap of undoped and Cu: ZnO thin films. The band gaps for each film are calculated by extrapolating the linear portion of the respective curve. It is found that the band gap value of undoped ZnO thin films was 3.28 eV. When Cu is doped into ZnO, the band gap decreases and found to be minimum 3.17 eV at 4% Cu: ZnO. This reduction in the band gap might be due to the position of Cu at nearby substitutional sites. Further, Cu doping might have introduced some additional energy levels in the ZnO near the valance band and conduction band edge, although the momentum of holes and electrons remain constant [32].

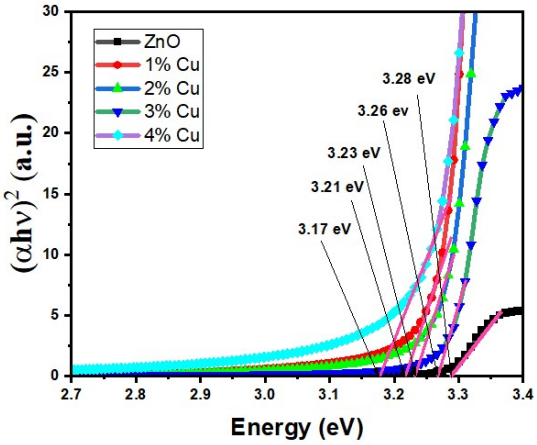

Figure 5: (color online) Bandgap of undoped and Cu doped ZnO.

3.5 Sensor application

The ZnO sensor experiences a change in resistance when gas molecules interact with its surface. In normal conditions, oxygen molecules are absorbed onto the ZnO surface and ionize into oxygen species by capturing electrons from the conduction band. This process creates a surface depletion layer, which increases the sensor's resistance [33]. When ethanol molecules come into contact with the ZnO surface, these oxygen species interact with the ethanol and release the trapped electrons back into the conduction band. Doping ZnO with Cu introduces additional charge carriers, typically in the form of holes or electrons which increases the material's conductivity.This modification enhances the material's

sensitivity by increasing the interaction strength between the target gas molecules and the sensing surface. Furthermore, the presence of Cu dopants alters the surface chemistry of ZnO, leading to improved selectivity by facilitating specific gas adsorption mechanisms.

Copper doping can alter the band structure of ZnO, potentially narrowing the band gap. These changes can improve electron mobility and facilitate the transfer of electrons when gas molecules interact with the sensor. which translates to higher sensitivity. Figure [6] shows the sensitivity measurements of undoped and Cu doped ZnO for ethanol vapor. The injection of ethanol is 1000 ppm for each sample. We have calculated the sensitivity of fabricated thin films by measuring the resistance in air (R_a) and in gas (R_e). When ZnO films are exposed to air, oxygen molecules are adsorbed on their surface by attracting an electron from the conduction band . Consequently, the resistance becomes high which may reduce conductivity. However, when ethanol gas is exposed to the film, gas reacts with the adsorbed oxygen ions on the surface of thin films and donates electrons back into the conduction band. As a result, conductivity increases compared to the undoped one. The optimum sensitivity of samples performed at the corresponding temperature is presented in Table [2]. It showed that the sensitivity increases with the increment in the Cu concentration. The sensitivity of pristine ZnO is only 16.57% at an operating temperature of 200 ^{0}. Conversely, the sensitivity of Cu: ZnO rises while increasing the Cu concentration. The maximum sensitivity of 70.60 % is found at Cu: ZnO (4%) at an operating temperature of 140 ^{0}, which is followed by 3%, 1% & 2% Cu: ZnO with the corresponding temperatures of 180 ^{0}, 200 ^{0} & 200 ^{0} respectively. The systematic decrease in operating temperature was observed from 200 C for undoped to 140 ^{0}for the 4% Cu: ZnO films.

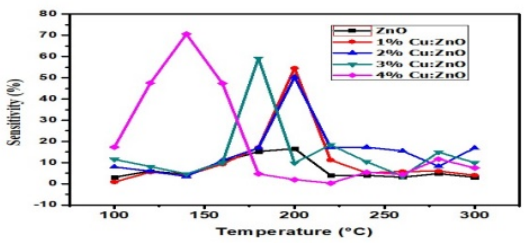

Figure 6: (colour online) Sensitivity of undoped and Cu: ZnO thin film with temperature variation.

Table 2: Maximum sensitivity of samples performed at various operating temperatures.

Sample	Maximum Sensitivity (%)	Operating Temperature (°C)
0% Cu:ZnO	16.57	200
1% Cu:ZnO	54.54	200
2% Cu:ZnO	50.29	200
3% Cu:ZnO	59.21	180
4% Cu:ZnO	70.60	140

As the Cu concentration increases, the crystalline size of the film slightly decreases, increasing the grain boundaries and surface roughness, which in turn increases the surface area, making it favorable for sensing applications. EDX analysis is used to determine the Cu wt.% in the elemental composition. In the case of 1% Cu doping in ZnO, it shows 4.25 wt.% of Cu, along with other elements, which leads to a significant enhancement in sensitivity from 16% to 54% towards ethanol vapor.

3.6 Sensing Mechanism

The ZnO sensor operates by detecting resistance changes caused by gas interactions with its surface. Under normal conditions, oxygen molecules are adsorbed on the ZnO surface, where they ionize into oxygen species by capturing electrons from the conduction band. This electron capture results in the formation of a surface depletion layer, which increases the sensor's resistance [33, 34]. When ethanol gas encounters the ZnO surface, the oxygen species react with the ethanol molecules, releasing the trapped electrons back into the conduction band. This electron return reduces the depletion layer, thereby lowering the sensor's resistance. The effectiveness of a gas sensor is influenced by factors such as sensitivity, selectivity, thermal stability, and response speed, which are largely determined by the shape, size, and surface morphology of the sensing material.

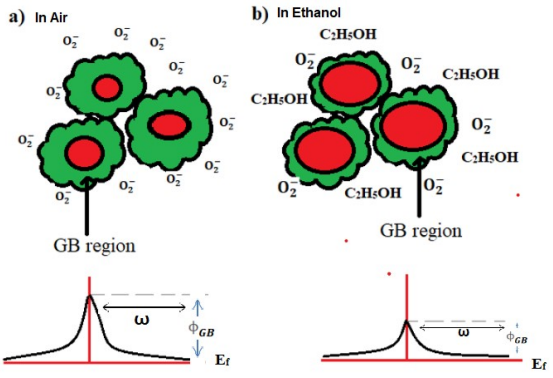

Figure 7: (color online) Depleted region at GB (a) under ambient condition (b) under ethanol condition.

In ZnO sensor, depleted layers are formed in in-

dividual nano-crystallites as well as in grain boundary (GB) regions due to the adsorption of oxygen molecules in ambient condition. Oxygen species from the atmosphere capture the electrons at the surface of ZnO, therefore, the negative charges would be trapped at the surface and grain boundary (GB) regions [Fig. 7]. Trapping of negative charge causes the band bending upward. As a result, GB potential (Φ_{GB}) and GB depletion width (ω) are formed which control the carrier transport through the GB region. In the presence of deoxidizing gas like ethanol, electrons trapped by oxygen molecules are returned the ZnO film and decreased potential (Φ_{GB}) and increased the conductivity [20, 25, 33].

4 Conclusion

This work concludes with the successful fabrication of undoped and Cu: ZnO thin films for ethanol sensing. The XRD results confirmed the polycrystalline hexagonal wurtzite structure of ZnO. EDAX values confirm the doping of Cu into the ZnO matrix. Likewise, SEM images showed that the as-prepared thin films are porous and grainy structured with the reduction of grain size for Cu doping film. The band gaps of Cu: ZnO significantly decreased with the increment of Cu concentration as compared to undoped ZnO. More importantly, when the Cu concentration was 4%, the maximum sensitivity of 70 % for ethanol exposure was at 140 ^0C. Based on these results, it can be concluded that Cu: ZnO holds significant potential in the field of gas sensing and might be useful to facilitate superior gas sensing performance, particularly in detecting ethanol vapor.

Acknowledgements

The authors would like to thank the International Science Program (ISP), Uppsala University, Sweden for supporting the Atmospheric and Material Science Research Group at the Department of Physics, Amrit Campus through NEP01 for conducting this work.

Declaration of Conflict of Interest

There is no known conflict of interest by the authors.

References

[1] B. P. J. D. L. Costello, R. J. Ewen, N. Guernion, and N. M. Ratcliff. Sens. actuators b. *Sens. Actuators B*, 87:207, 2002.

[2] F. Paraguay-Delgado, M. Miki-Yoshida, J. Morales, and W. Estrade. Thin solid films. *Thin Solid Films*, 373:137, 2000.

[3] P. Ivanov, E. Llobet, X. Vilanova, J. Brezmes, J. Hubalek, and X. Coreig. Sens. actuators b. *Sens. Actuators B*, 99:201, 2004.

[4] N. Asif, M. Amir, and T. Fatma. Bioprocess and biosystems engineering. *Bioprocess and Biosystems Engineering*, 46:1377–1398, 2023.

[5] S. Vyas. Johnson matthey technology review. *Johnson Matthey Technology Review*, 64:202–218, 2020.

[6] X. L. Cheng, H. Zhao, L. H. Huo, S. Gao, and J. G. Zhao. Sens. actuators b. *Sens. Actuators B*, 102:248, 2004.

[7] T. Yasutaka, K. Masaaki, K. Akiko, M. Hideki, and O. Yutaka. Jpn. j. appl. phys. *Jpn. J. Appl. Phys.*, 33:6611, 1994.

[8] C. Y. Lu, S. P. Chang, S. L. Chang, T. J. Hsueh, C. L. Hsu, Y. Z. Chiou, and I. C. Chen. Ieee sens. j. *IEEE Sens. J.*, 9(4), 2009.

[9] N. H. Hashim, S. Subramani, and M. Devarajan. *J. Aust. Ceram. Soc.*, 53:421–431, 2017.

[10] I. Stambolova, K. Konstantinov, S. Vassilev, P. Pesheu, and T. Tsacheva. *Mater. Chem. Phys.*, 63:104, 2000.

[11] T. Jun, M. Tomoki, M. Shigenori, M. Norio, and Y. Noboru. *Chem. Lett.*, 19(3):477, 1990.

[12] R. S. Bisht, R. R. Ghimire, and A. K. Raychaudhuri. *The Journal of Physical Chemistry C*, 119(49):27813–27820, 2015.

[13] H. Nanto, T. Minami, and S. Takata. *J. Appl. Phys.*, 60:482, 1986.

[14] I. Stambolova, V. Blaskov, M. Shipochka, S. Vassilev, V. Petkova, and A. Laukanov. *Materials Science and Engineering B*, 177(13):1029–1037, 2012.

[15] A. M. Pineda-Reyes, M. R. Herrera-Rivera, H. Rojas-Chavez, H. Cruz-Martinez, and D. I. Medina. *Sensors*, 21:4425, 2021.

[16] M. Poloju, N. Jayababu, and M. V. R. Reddy. *Materials Science and Engineering B*, 227:61–67, 2018.

[17] D. Aryanto, W. N. Jannah, Masturi, T. Sudiro, A. S. Wismogroho, P. Sebayang, and P. Marwoto. *Journal of Physics: Conference Series*, 817:012025–012032, 2017.

[18] J. Y. Son, S. J. Lim, J. H. Cho, W. K. Seong, and H. Kim. *Appl. Phys. Lett.*, 93(5):053109, 2008.

[19] D. D. Mulmi, A. Dhakal, and B. R. Shah. *Nepal Journal of Science and Technology*, 15:111–116, 2014.

[20] R. R. Ghimire, B. P. Pokhrel, S. P. Gupta, L. P. Joshi, and K. B. Rai. *Journal of Nepal Physical Society*, 9(1):73–82, 2023.

[21] M. M. Rahman, A. Jamal, S. B. Khan, and M. Faisal. *ACS Appl. Mater. Interfaces*, 3:1346, 2011.

[22] D. Sivalingam, J. B. Gopalkrishnan, and J. B. B. Rayappan. *Sens. Actuators B*, 166:624, 2012.

[23] G. Vijayaprasath, R. Murugan, G. Ravi, T. Mahalingam, and Y. Hayakawa. *Appl. Surf. Sci.*, 313:870, 2014.

[24] J. B. Baxter and E. S. Aydil. *Sol. Energy Mater. Sol. Cells*, 90:607, 2006.

[25] N. Neupane, R. Ghimire, D. R. Gibbs, S. P. Shrestha, S. Dhakal, D. D. Mulmi, and L. Pradhan Joshi. *Journal of Nepal Physical Society*, 9(2):7–13, 2023.

[26] L. P. Joshi, B. V. Khatri, S. Gyawali, S. Gajurel, and D. K. Chaudhary. *J. Phys. Sci.*, 32(2):15–26, 2021.

[27] M. Oztas and M. Bedir. *Thin Solid Films*, 516(8):1703, 2008.

[28] M. Laurenti and V. Cauda. *Coatings*, 8(2):67–91, 2018.

[29] N. Narayanan and D. N. Kannoth. *Journal of Materials Science: Materials in Electronics*, 28:5962–5970, 2017.

[30] C. M. Vladut, S. Mihaiu, E. Tenea, S. Preda, J. M. Calderon-Moreno, M. Anastasescu, H. Stroescu, I. Atkinson, M. Gartner, C. Moldovan, and M. Zaharescu. *Journal of Nanomaterials*, 2019:1–13, 2019.

[31] C. Kittel. *Introduction to Solid State Physics*. John Wiley and Sons, New York, USA, 8th edition, 1986.

[32] J. M. Ziman. *Principles of Theory of Solids*. Cambridge University Press, Cambridge, 2nd edition, 1972.

[33] D. K. Chaudhary, Y. S. Maharjan, S. Shrestha, S. Maharjan, S. P. Shrestha, and L. P. Joshi. *J. Phys. Sci.*, 33(1):97–108, 2022.

[34] K. Ozawa, T. Hasegwa, K. Edamoto, K. Takahansi, and M. Kamada. *J. Phys. Chem. B*, 106(36):9380–9386, 2002.